



## Research article

# Physicochemical and biological assessment of silver nanoparticles immobilized Halloysite nanotubes-based resin composite for dental applications

Tejas Barot, Deepak Rawtani<sup>\*</sup>, Pratik Kulkarni

Gujarat Forensic Sciences University, Nr. DFS Head Quarters, Sector 9, Gandhinagar, Gujarat, 382007, India

## ARTICLE INFO

## Keywords:

Materials science  
Dental composites  
Silver nanoparticle  
Halloysite nanotubes  
Mechanical properties  
Antimicrobial activity  
Cytotoxicity

## ABSTRACT

**Objective:** The purpose of this study was to investigate the effect of Silver nanoparticle immobilized Halloysite Nanotubes (HNT/Ag) fillers on physicochemical, mechanical, and biological properties of novel experimental dental resin composite in order to compare with the properties of corresponding composites containing conventional glass fillers.

**Methods:** Dental resin (Bis-GMA/TEGDMA with ratio 70/30) composites were prepared by incorporation of varied mass fraction of HNT/Ag. Experimental composites were divided into six groups, one control group and five experimental groups containing mass fraction 1 to 10.0 wt. % of HNT/Ag. Mechanical properties of the dental composites were recorded. Degree of conversion and depth of cure of the dental resin composites were assessed. Antimicrobial properties were assessed using agar diffusion test and evaluation of cytotoxicity were performed on NIH-3T3 cell line.

**Results:** The inclusion of mass fractions (1–5 wt. %) of the HNT/Ag in dental resins composites, significantly improved mechanical properties. While, addition of larger mass fractions (7.5 and 10 wt. %) of the HNT/Ag did not show further improvement in the mechanical properties of dental resins composites. These composites also demonstrated satisfactory depth of cure and degree of conversion. A significant antibacterial activity was observed on *S. mutans*. No significant cytotoxicity was found on NIH-3T3 cell lines.

**Conclusion:** The incorporation of HNT/Ag in Bis-GMA/TEGDMA dental resins composites resulted in enhancement in mechanical as well as biological properties for dental applications.

**Clinical significance:** HNT/Ag containing dental composite is proposed to be highly valuable in the development of restorative dental material for patients with high risk of dental caries.

## 1. Introduction

Resin-based composites have been used as dental restorative materials because of their numerous benefits such as provision of great aesthetics, good manoeuvrability and biocompatibility [1]. Resin based dental composites are constantly studied with the help of advanced technology to increase their mechanical strength and life span. According to several reports, the integration of inorganic fillers in resin composite could enhance their mechanical properties, thereby increasing the clinical performance [2, 3, 4].

Unfortunately, the success of a commercially available dental composite still poses a great challenge due to their limitation such as poor mechanical properties, low wear resistance, and no inherent antibacterial

activity. These resin-based composites are being explored continuously through advanced technologies to enhance as well as heighten their clinical performance. One of the factors affecting the life of dental filling is the secondary caries, oral biofilm formation and proliferation of bacterial colonies beside the margins of dental filling and eventually a failure of the restoration [5]. *Streptococcus mutans* (*S. mutans*) is recognized as one of the primary bacterial species responsible for secondary caries.

The application of nanotechnology for developing advanced dental materials has led to a great impact in dental biology. Fabrication of dental resin composite with antibacterial nano fillers is necessary which can increase their performance and lifespan by resisting oral biofilm formation [6]. Uniform distribution of the nanoparticles in resin matrix plays

<sup>\*</sup> Corresponding author.

E-mail address: [rawtanid@gmail.com](mailto:rawtanid@gmail.com) (D. Rawtani).

the important role in the life span enhancement of the dental resin composites [7].

Halloysite nanotubes (HNTs) is an inexpensive naturally occurring clay mineral with a tubular structure [8]. The lengths of HNTs are usually in the range from ~100 nm to 1–2  $\mu\text{m}$  and the diameters are usually in nanometers. Furthermore, the benefits associated with halloysite such as non-toxicity, biocompatibility, high mechanical strength, easy processing and purification make it a potential reinforcing filler for the development of a dental composite [9, 10]. As HNT does not inherit any antibacterial properties thus, attachment of an antibacterial agent to halloysite can create a novel antibacterial filler.

Noble metal nanoparticles (NP) exhibit unique optical, catalytic and antibacterial properties [11]. Addition of noble metal NPs with antibacterial properties in dental resins matrix yields novel dental composites and also prevent attachment and proliferation of oral micro-organisms on tooth surface [12]. Since decades silver is a well-established antibacterial agent which has been used in different medical procedures such as burn care, wound dressings, oral and skin infections etc. [13, 14]. Silver ions exhibits a broad-spectrum antibacterial activity against both gram-positive and gram-negative bacterial species [15]. Properties of Silver nanoparticles (AgNPs) such as their Nano size, high antibacterial activity and inexpensive fabrication can be beneficial in numerous biological applications. By virtue of silver NPs' antimicrobial potential, AgNPs containing dental fillers could provide antibacterial properties to the resultant dental resin based composites [16, 17]. However, direct incorporation of AgNPs in resin-based composite could lead to a rapid leaching of nanoparticles as well as reduction of their antimicrobial potential. This problem can be minimized by attaching AgNPs directly to nanotubes and control the quick release of antimicrobial agent [18, 19, 20, 21].

The focus of this study is to evaluate the potential of silver NP immobilized Halloysite Nanotubes (HNT/Ag) filler on the physico-chemical and biological properties of a resultant dental resin composite along with the comparison of their mechanical properties by addition of conventional glass fillers, with total filler load maintained at 70 wt.%. The surface morphologies were observed under Scanning Electron Microscope (SEM) and Transmission Electron Microscope (TEM). *Streptococcus mutans* (*S. mutans*) was used for evaluating the antibacterial activity and cytotoxicity was performed on NIH-3T3 cell lines for HNT/Ag incorporated Bis-GMA/TEGDMA dental resin composites.

## 2. Materials and methods

### 2.1. Materials

Bis-GMA (Bisphenol A glycerolate dimethacrylate), TEGDMA (Tri (ethylene glycol) dimethacrylate, 95%) and conventional dental glass filler (V-117-1190) (silanized barium borosilicate glass powder) was provided by the Esstech Co. (Essington, PA). CQ (Camphorquinone, 97%), 4-EDMAB (Ethyl-4-dimethylaminobenzoate, 99%) were bought from TCI Chemicals (India) Pvt Ltd. Purified Halloysite powder (1250 mesh), Silver nitrate ( $\text{AgNO}_3$ , 99.9%) and Sodium borohydride ( $\text{NaBH}_4$ ) were purchased from Sigma-Aldrich. Other reagents required for the study, including APTES (3-aminopropyl) triethoxysilane) (97%) and Toluene was acquired from TCI Chemicals (India) Pvt Ltd. Milli-Q water was used for all experiments.

### 2.2. Methods

#### 2.2.1. Functionalization of HNT with APTES

Organosilane modified HNTs were prepared by previously reported protocol with some modifications. First, a 25 mL of APTES was dissolved in a beaker containing toluene. Thereafter, 2.5 g of HNTs was added in the solution mixture. Then mixture was kept under ultra-sonication for 30 min. The reaction solution was kept under constant stirring for 24 h at 70 °C. The resultant precipitated HNTs obtained after 24 h was

thoroughly washed with toluene to eliminate the excess organosilane and dried for 48 h at room temperature [20].

#### 2.2.2. Immobilization of silver nanoparticles (AgNPs) on Halloysite nanotubes

The immobilization of AgNPs on HNTs were carried using  $\text{AgNO}_3$  as silver precursor. Milli-Q water was used to prepare a 20 mL  $10^{-2}$  M  $\text{AgNO}_3$  solution. Functionalized HNT (fHNT) was added into Milli-Q water and the mixture was magnetically stirred continuously to obtain a homogenous dispersion. Thereafter, 2 mL of  $\text{AgNO}_3$  solution (0.2 M) was added slowly to the mixture and stirred for 5 h at room temperature to complete immobilization and then reduced using 2 mL of a freshly prepared cold  $\text{NaBH}_4$  (0.1 M) solution. The Silver nanoparticles immobilized nanotubes were recovered by centrifugation, washed with Milli-Q water several times to remove the excess borohydride and stored for further evaluations (Figure 1) [21–23].

#### 2.2.3. Preparation of dental resin composites

The detailed composition of HNT/Ag fillers in dental resin composites are shown in Table 1. For resin preparation, Bis-GMA and TEGDMA were used. These monomers were mixed in ratios of 69.5 and 29.5 respectively. 0.5 wt. % CQ and 0.5 wt. % 4-EDMAB were added as photoinitiators to the mixture [24, 25] (Table 1).

Six groups of experimental resin composite samples were made: one control group, and five groups with different mass fractions {H1 (0%), H2 (1%), H3 (2.5%), H4 (5%), H5 (7.5%) and H6 (10%)} of HNT/Ag in each group. The conventional dental glass fillers were further mixed with different mixtures of resin HNT/Ag, with overall filler load maintained at 70 wt. % to prepare dental composites. The detailed composition of HNT/Ag with conventional dental glass fillers in dental resin composites are shown in Table 2.

The HNT/Ag were added in the TEGDMA and mechanically stirred for 1h at 300 rpm. Bis-GMA, CQ and 4-EDMAB were added simultaneously and mixture was mechanically stirred at 300 rpm for 30 min more. The composite mixtures were reserved in a vacuum chamber at room temperature overnight to allow sufficient time for the monomers to infiltrate the nanotubes and removal of residual air bubbles. Subsequently, the HNT/Ag incorporated composite mixture was inserted into the suitable silicon rubber molds covered by glass slides, and polymerized with Woodpecker i-LED curing unit (430–490 nm, Guilin Woodpecker Medical Instrument Co Ltd, China) for 40 s on both side. The distance between the sample surface and the light tip was kept at 5 mm [26]. The maximum amount of HNT/Ag fillers in the resin was limited to 10%. The resultant dental resin composite samples were polished with silicon carbide abrasive papers (P1500 grit) and stored in dark room before evaluation.

### 2.3. Characterization

#### 2.3.1. Characterization of inorganic fillers

##### (1) Scanning Electron Microscope (SEM)

Morphological observations of HNT, fHNT and experimental fractured surfaces of composites comprising varied mass fractions of HNT/Ag were evaluated on Scanning Electron Microscope (SEM, Zeiss EVO 18, USA). Elemental analysis of HNT/Ag was measured by energy-dispersive X-ray fluorescence analysis (EDXRF). For the analysis, all the specimens were fixed on specific stubs and vacuum coated with Palladium–Gold film to avoid charge accumulation.

##### (2) Transmission Electron Microscope (TEM)

Morphological observations of HNTs and Silver nanoparticle immobilized Halloysite Nanotubes (HNT/Ag) were conducted on Transmission Electron Microscope (TEM, FEI Technai G2 F30 model) to confirm the loading of AgNPs on fHNT surface, at an accelerating voltage of 300 kV.

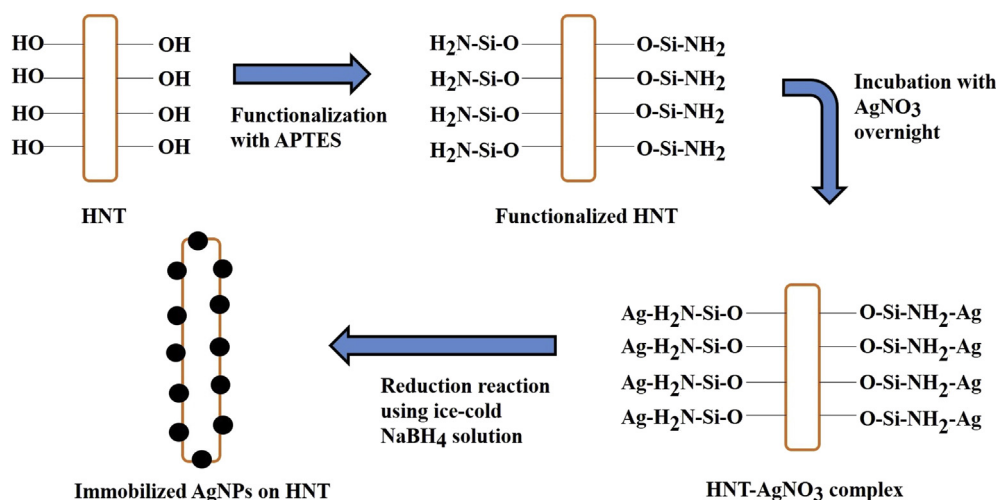


Figure 1. Schematic illustration of the Halloysite nanotubes and AgNPs reaction.

Table 1. Composition of HNT/Ag containing different composite groups used in this study.

Groups composite	% wt. of HNT/Ag	Resin (matrix)	Other component
H1-Control	0%	Bis-GMA/TEGDMA 70/30 wt.%	CQ <sup>a</sup> 0.5 wt.%, 4-EDMAB <sup>b</sup> 0.5 wt.%
H2	1%	Bis-GMA/TEGDMA 70/30 wt.%	CQ <sup>a</sup> 0.5 wt.%, 4-EDMAB <sup>b</sup> 0.5 wt.%
H3	2.5%	Bis-GMA/TEGDMA 70/30 wt.%	CQ <sup>a</sup> 0.5 wt.%, 4-EDMAB <sup>b</sup> 0.5 wt.%
H4	5%	Bis-GMA/TEGDMA 70/30 wt.%	CQ <sup>a</sup> 0.5 wt.%, 4-EDMAB <sup>b</sup> 0.5 wt.%
H5	7.5%	Bis-GMA/TEGDMA 70/30 wt.%	CQ <sup>a</sup> 0.5 wt.%, 4-EDMAB <sup>b</sup> 0.5 wt.%
H6	10%	Bis-GMA/TEGDMA 70/30 wt.%	CQ <sup>a</sup> 0.5 wt.%, 4-EDMAB <sup>b</sup> 0.5 wt.%

<sup>a</sup> Camphorquinone.

<sup>b</sup> Ethyl-4-dimethylaminobenzoate.

The samples were dispersed in n-propanol for 5 min through ultrasonication. During sonication, a small droplet of the solution was taken and placed gently over a carbon coated copper grid [27]. The grid was settled for 5 min and used for TEM examination.

### (3) X-ray diffraction (XRD) analysis.

X-ray diffraction patterns of HNT, fHNT, Ag NPs and HNT/Ag were recorded using CuK $\alpha$  radiation ( $\lambda = 1.54 \text{ \AA}$ ) of a GNR APD 2000 PRO diffractometer. The instrument was operated at 30 mA and 40 kV. 600 mg of the dry sample powder was placed on the sample holder and placed in the instrument for analysis. XRD data was recorded from  $10^\circ$  to  $80^\circ$  (2 $\theta$ ) at a scanning speed of  $1 \text{ min}^{-1}$ .

### (4) Fourier transform-infrared (FTIR) analysis.

The vibrational spectra of HNT, fHNT and HNT/Ag were obtained using FTIR-JASCO 4100. The samples were mixed with potassium

bromide (KBr) in a 1:100 ratio, finely ground and the pellet was prepared using a pellet press. For the recording the background spectrum, a blank KBr pellet was used. The vibrational spectral range for sample analysis was kept fixed at  $4000\text{--}400 \text{ cm}^{-1}$  wavenumber by 32 scans, and at  $4 \text{ cm}^{-1}$  resolutions [28].

### 2.3.2. Characterization of dental composites

#### (1) Mechanical properties.

The Flexural Strength (FS), Flexural Modulus (FM) and Compressive Strength (CS) of HNT/Ag incorporated dental resin composites were assessed by Universal Testing Machine (Lloyd LRX, UK). The rectangular-shaped specimens ( $25 \text{ mm} \times 2 \text{ mm} \times 2 \text{ mm}$ ) were fabricated from composite paste and polymerized with LED curing unit for 40 s according to ANSI/ADA specification NO. 27- 2009 (ISO-4049). Flexural Strength (FS) and Flexural Modulus (FM) of the polymerized specimens were measured by a three-point bending test with 20 mm span and 1 mm/min

Table 2. Composition of HNT/Ag and conventional dental glass fillers containing different composite groups used in this study.

Sample code	% wt. of HNT/Ag	% wt. of Glass fillers	Resin (matrix)	Other component
G1-Control	0	70	Bis-GMA/TEGDMA 70/30 wt.%	CQ <sup>a</sup> 0.5 wt.%, 4-EDMAB <sup>b</sup> 0.5 wt.%
G2	1	69	Bis-GMA/TEGDMA 70/30 wt.%	CQ <sup>a</sup> 0.5 wt.%, 4-EDMAB <sup>b</sup> 0.5 wt.%
G3	2.5	67.5	Bis-GMA/TEGDMA 70/30 wt.%	CQ <sup>a</sup> 0.5 wt.%, 4-EDMAB <sup>b</sup> 0.5 wt.%
G4	5	65	Bis-GMA/TEGDMA 70/30 wt.%	CQ <sup>a</sup> 0.5 wt.%, 4-EDMAB <sup>b</sup> 0.5 wt.%
G5	7.5	62.5	Bis-GMA/TEGDMA 70/30 wt.%	CQ <sup>a</sup> 0.5 wt.%, 4-EDMAB <sup>b</sup> 0.5 wt.%
G6	10	60	Bis-GMA/TEGDMA 70/30 wt.%	CQ <sup>a</sup> 0.5 wt.%, 4-EDMAB <sup>b</sup> 0.5 wt.%

<sup>a</sup> Camphorquinone.

<sup>b</sup> Ethyl-4-dimethylaminobenzoate.

cross-head speed using a UTM. The flexural strength was calculated as per 3PL/2bd<sup>2</sup> equation, where P = load at fracture; L = span length; b = width; and d = thickness [29]. For the Compressive Strength (CS) assessment, cylindrical specimens ( $\Phi$  4 mm  $\times$  6 mm) were created and evaluated as above, with a cross-head speed of 1 mm/min.

## (2) Degree of conversion.

FTIR spectrometer (FTIR-JASCO 4700), equipped with an attenuated total reflectance crystal (ATR) was used to examine degree of conversion (DC) of experimental dental resin composites. The spectral range was fixed at 4000–400  $\text{cm}^{-1}$  with 32 scans, and at 4  $\text{cm}^{-1}$  resolutions for analysis [30]. FT-IR spectra were recorded before and after curing of each composite specimen. Also, DC of every dental resin composite was found from the ratio of absorbance intensities of aliphatic C–C bond (1638  $\text{cm}^{-1}$ ) against internal standard of aromatic C–C bond (1608  $\text{cm}^{-1}$ ). The tests were performed in triplicates for each composite sample. The DC (%) was calculated from formula (1):

$$DC(\%) = \left(1 - \frac{R_{\text{cured}}}{R_{\text{uncured}}}\right) \times 100 \quad (1)$$

where R = band height at 1638  $\text{cm}^{-1}$ /band height at 1608  $\text{cm}^{-1}$ .

## (3) Curing depth.

The silicon rubber mould with ( $\Phi$  4 mm  $\times$  10 mm) dimension was packed uniformly with composite paste, irradiated vertically for 30 s with the LED curing unit as per ISO 4049 guidelines [30]. The sample was demoulded, and uncured material was scraped from bottom with a spatula. The curing depth of specimen was measured via digital caliper for 5 times ( $n = 3$ , accurate to 0.01 mm) at several angles. As per ISO guideline, the obtained value was divided by 2 to get the final curing depth value.

## (4) Antimicrobial activity.

*Staphylococcus mutans* (*S. mutans*, MTCC 890) was used as a model organism to evaluate the antibacterial activity of HNT/Ag resin composites at different compositions [31]. Disk diffusion method was used under aseptic condition to measure *S. mutans* inhibition. The test specimens for HNT/Ag resin composites were 6 mm in diameter and 2 mm in thickness. The specimens were fabricated by inserting the respective materials into the rubber mould over a glass slab place in between 2 Mylar strips. The composite material was polymerized with LED light for 40 s on both side. The lyophilized culture of *S. mutans* strains were acquired from Institute of Microbial Technology, Chandigarh. They were grown in 15 mL of Luria Bertani broth (HI Media Laboratory Pvt. Ltd., India) individually for 48 h at 37 °C. The resultant bacteria were placed in 5 ml of Brain Heart Infusion broth again (HI Media Laboratory Pvt. Ltd., India) for 24 h at 37 °C to form a suspension, consistent to 10<sup>6</sup> CFU/mL using the McFarland scale. All polymerized specimens were immersed in 10 mL of 100% methanol and washed with agitation for 1 h to remove any non-polymerized materials and for sterilization Ethylene oxide gas was used [32].

For the disk diffusion test, a base layer comprising 15 ml Brain Heart Infusion agar (HI Media Laboratory Pvt. Ltd., Mumbai, India) was uniformly spread to a thickness of 5 mm in sterile petri dish. After solidification of the culture medium, 6 mm wells were made using the sterile borers in each petri dish [33]. A maximum of 4 specimens per plate were used. The culture plates were placed in the incubator for 24 h at 37 °C. After 24 h incubation, the plates were observed for uniform culture growth (granular, frosted glass appearance) and inhibition zones formation around the discs that was measured in millimeters. The mean of three measurements of the diameter of each inhibition zone for each disk was calculated. The trial was performed in triplicates [33].

## (5) In-vitro cytotoxicity test.

NIH-3T3 cell line was used to evaluate the cytotoxicity of experimental HNT/Ag resin dental composites. Optimal number (nearly 5000 cells per well) of NIH-3T3 cells in 100  $\mu\text{L}$  media were seeded in 96 well plates. Cells were cultured in Minimal Essential Medium (MEM) supplemented with 10% Fetal Bovine Serum (FBS), penicillin (100 U/ml) and streptomycin (100  $\mu\text{g}/\text{mL}$ ). The cells were incubated at 37 °C in CO<sub>2</sub> incubator for 24 h. After 24 h, when cells attained confluence of around 40–50%, were treated with dental composite samples in triplicate. The plates were again kept in CO<sub>2</sub> incubator for 24 h, 48 h and 72 h at 37 °C. Every 24 h, Photographs were also taken. Subsequently, 10  $\mu\text{L}$  of MTT (5 mg/mL) was added in each well in the media. After incubating for 3 h at 37 °C in 5% CO<sub>2</sub> incubator set, the plate was observed for formed formazan crystals under the microscope. Media was discarded without disturbing formazan crystals. 200  $\mu\text{L}$  of DMSO was added per well to solubilize the crystals. Plate was incubated on a shaker in dark for 10 min. Absorbance at 570 nm was read. IC50 values were calculated for each sample [34, 35].

### 2.3.3. Statistical analysis

The results of FS, FM, and CS were evaluated with one-way analysis of variance (ANOVA) using 20<sup>th</sup> version of SPSS software (USA). References to substantial differences were based on a probability of  $p < 0.05$  unless otherwise stated.

## 3. Results

### 3.1. Morphological evaluation

The ultra-structural and morphological study of the HNTs with SEM has been represented in Figure 2. SEM images clearly show the cylindrical shaped tubes of HNTs with an open-ended lumen. SEM image of fhNT shows coating of APTES on outer surface of HNT post-surface functionalization (Figure 2). The EDXRF spectra shows the characteristic peak of Al, Si and Ag in HNT/Ag composites. Halloysite nanotubes are mainly composed of SiO<sub>2</sub> and Al<sub>2</sub>O<sub>3</sub> due to the presence of these metal with ratio of 1.33 respectively. EDXRF spectra shows a characteristic peak of the aluminum peak at 1.76 keV and silver at 2.97 keV. The extra Silver peak in the acquired spectra of EDXRF confirms the successful formation of HNT/Ag.

The morphology of HNTs and HNT/Ag were observed through Transmission Electron Microscopy (TEM). As shown in Figure 3, the Halloysite Nanotubes showed a uniform dispersion. The inner and outer diameter of the nanotubes were 30–50 nm and 70–120 nm respectively along with a typical length of the tube ranging between 1.0–1.5  $\mu\text{m}$ . HNTs were seen as cylindrical tubes with a transparent central area. The outer diameter of the nanotubes increases marginally after surface functionalization with APTES signifying coating of the nanotubes with amine groups [20, 27]. The morphology of HNT/Ag demonstrated that the cylindrical shaped nanotubes were immobilized with spherical AgNPs, having particle size of 10–15 nm. The dark spots in Figure 3c could be attributed to AgNPs immobilized on the outer surface of the HNT. All the AgNPs are evenly distributed over the outer surface of the nanotubes devoid of any agglomeration. Owing to its unique structure, HNT has been reckoned as a promising nanocarrier for the immobilization of biologically active molecules [36, 37] (Figure 3).

### 3.2. X-ray diffraction of HNT, fhNT, HNT/Ag and AgNPs

The crystals structures of HNT, fhNT, HNT/Ag and AgNPs were characterized by XRD. The results showed that HNT exhibits diffraction peaks at  $2\theta$  values of 11.9°, 19.9° and 24.91°, which correspond to the (001), (020/110) and (002) basal plane present in its crystalline structure [27, 38]. The results of fhNT demonstrated its characteristic peaks at 11.9°, 19.9° and 24.91° in  $2\theta$ , however lack of any new peak in the XRD

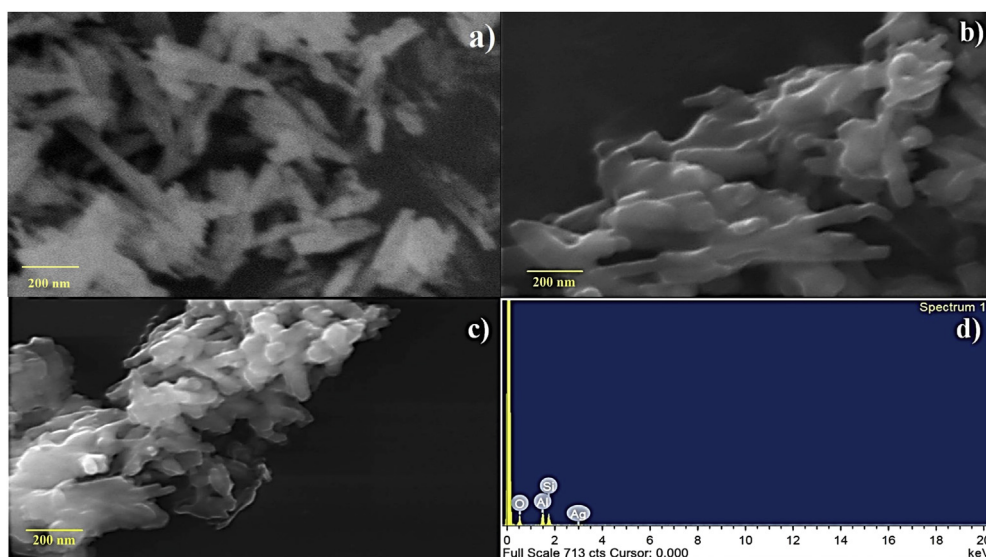


**Figure 2.** (a) Representative SEM images of the Halloysite nanotubes (HNTs); (b) and (c) Representative SEM images of functionalized Halloysite nanotubes (fHNT); (d) Representative EDXRF spectra of Silver nanoparticles immobilized Halloysite Nanotubes (HNT/Ag).

pattern of fHNT shows the modification by APTES does not affect the structure of HNTs. Ag NPs showed peaks at  $38.19^\circ$ ,  $65.71^\circ$  and  $77.70^\circ$  which are the characteristic peaks of Silver [39]. The newly emerged diffraction peaks of the HNT/Ag at  $38.19^\circ$  (100),  $65.71^\circ$  (220), and  $77.70^\circ$  (311) confirmed the attachment of Ag NPs on fHNT (Figure 4).

### 3.3. FTIR analysis of HNT, fHNT, Ag NPs and HNT/Ag

FTIR spectra showed the vibrational spectra for the HNT, fHNT and HNT/Ag in the range of  $4000\text{--}400\text{ cm}^{-1}$  in Figure 5. Specific absorption bands at  $911$  and  $3695\text{ cm}^{-1}$  due to Al–O–OH bending and O–H stretching confirm the presence of HNT [27]. A specific in-plane stretching vibration in HNT found at  $1091\text{ cm}^{-1}$  and  $1032\text{ cm}^{-1}$  was due to presence of Si–O–Si. In addition, new peaks observed at  $1483$ ,  $1672$ ,  $2937$  and  $3627\text{ cm}^{-1}$  of fHNT are attributed to the Si–C deformation, N–H deformation, C–H (stretching), and the N–H (stretching) functional groups respectively [27, 40]. The vibration band of HNT/Ag at  $1400\text{ cm}^{-1}$  could indicate the interaction between Ag NPs with fHNT at Si–C deformation. However, an alteration in frequencies associated with

the OH functional group of fHNT and a noticeable wave number at  $3626\text{ cm}^{-1}$  (OH stretching),  $910\text{ cm}^{-1}$  and  $1034\text{ cm}^{-1}$  (C–OH bending) evidently indicates the interaction of OH groups with Ag NPs [40, 41]. Additionally, fHNT shows peaks at  $1110\text{ cm}^{-1}$ ,  $1020\text{ cm}^{-1}$  and after the attachment of AgNPs with fHNT these peaks merged and shows the combined peaks at  $1034\text{ cm}^{-1}$  [27, 40 and 41] (Figure 5).

### 3.4. Properties of dental resin composites

#### 3.4.1. Mechanical characterization

The mechanical properties of dental composites incorporated with HNT/Ag fillers and corresponding dental composites incorporated with both HNT/Ag and conventional dental glass filler were measured and the results are displayed in Figure 6. The nanotube based fillers significantly increased the values of FS, FM and CS of dental composites ( $p < 0.05$ ). It is clearly seen that the mechanical properties of the resin composites were influenced by the amount of fillers in resin matrix. As shown in Figure 6, the values of FS, FM and CS were significantly increased upon the inclusion of varied mass fractions of HNT/Ag into the dental

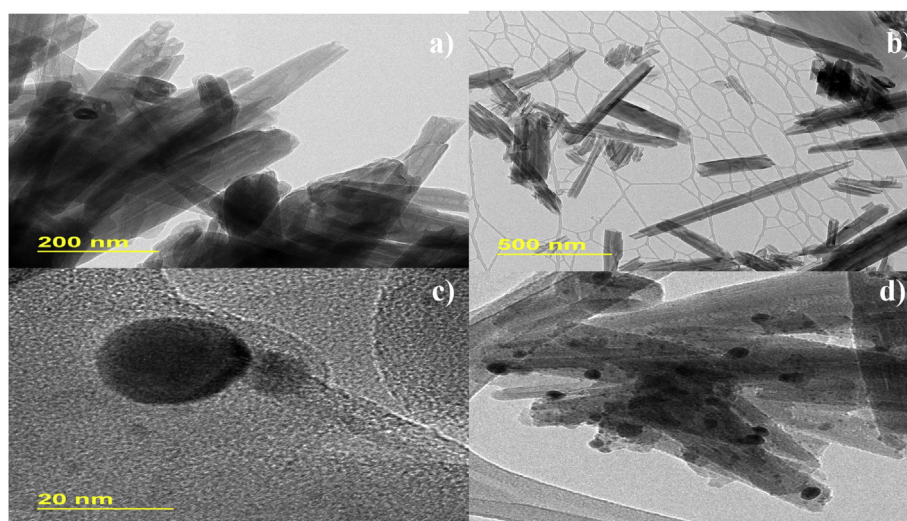


**Figure 3.** (a) and (b) representative TEM micrographs of the Halloysite nanotubes (HNTs); (c) representative TEM micrograph of a single Silver NP on HNT/Ag surface and (d) representative TEM micrograph of the HNT/Ag.

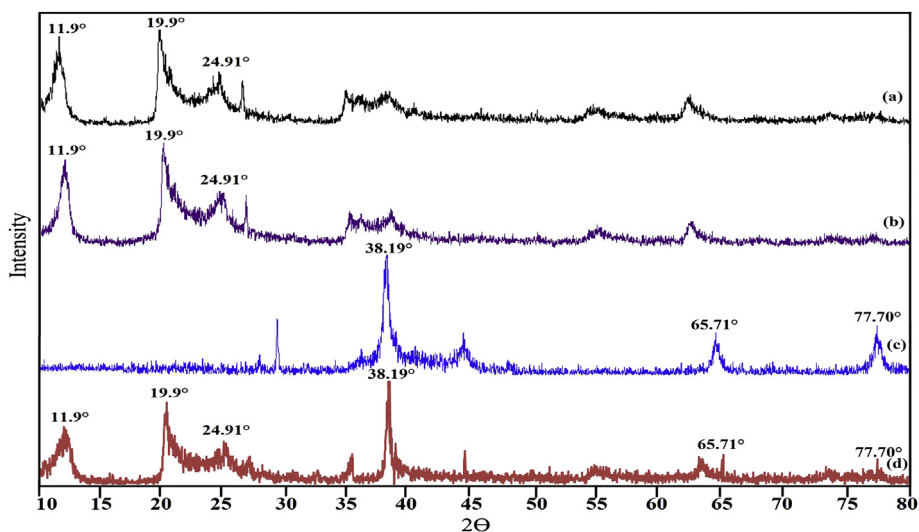


**Figure 4.** X-ray diffraction patterns of (a) Halloysite Nanotubes (HNTs); (b) functionalized Halloysite Nanotubes (fHNT); (c) Silver NP immobilized HNT (HNT/Ag); (d) Silver NPs (Ag NPs).

composite (without glass filler) compared to the control group (H1). The control group (H1) displayed average FS, FM and CS values - 86.5 MPa, 4.1 GPa and 182.2 MPa respectively. All the composites with HNT/Ag achieved higher FS, FM and CS values than the control group (H1). With the increase in the filler amount from 1% to 5 %, the mechanical properties also increased. The 5% HNT/Ag (H4) showed the best flexural strength ( $133.40 \pm 2.15$  MPa), flexural modulus ( $5.7 \pm 0.46$  GPa) and compressive strength ( $278.60 \pm 2.20$  MPa) which were substantially higher than the control group. The flexural strength and modulus started decreasing as the ratio of HNT/Ag were increased to 7.5% and 10 wt. %, which may be due to the agglomeration formed by HNT/Ag. A higher amount of filler in resin composites leads to aggregation of HNT/Ag causing loss of mechanical properties. These findings were in accordance with earlier reports stating the same [44]. Thus, a lower filler concentration (5 % wt.) was found to be optimum for the study (Figure 6).

The corresponding composites with both HNT/Ag and conventional glass filler also demonstrated enhancements of mechanical properties of the experimental dental resin composites. The resin composites filled with 5% of HNT/Ag (G4) displayed higher FS, FM than the control group

resin, however, the composites filled with 7.5% (G5) and 10% (G6) of the HNT/Ag had lesser FS and FM values than 5% of HNT/Ag (G4) group resin. These results showed that higher mechanical strength would not be attained at higher mass fractions of HNT/Ag, which may be due to the agglomerate formation that causes mechanical weakening in resin [43].

#### 3.4.2. Degree of conversion

The DC of the dental composites was evaluated by FTIR-ATR. Insignificant decrease was observed with the inclusion of HNT/Ag with a concentration ratio of 1–10% compared to the control group. The DC of different mass fraction of HNT/Ag dental composites varied from 71 to 66%. The DC for all the resin composites groups, after light curing remained high. On observation, it was found that the composites containing HNT/Ag had negligible difference in respect to the composites containing conventional dental glass fillers and HNT/Ag. These results were also in accordance with some previous reports [44, 46] (Figure 7).

The greater conversion of double bonds of monomer is essential for high mechanical strength of dental composites. Converted double bonds strengthen effects of composites thus resulting in higher mechanical

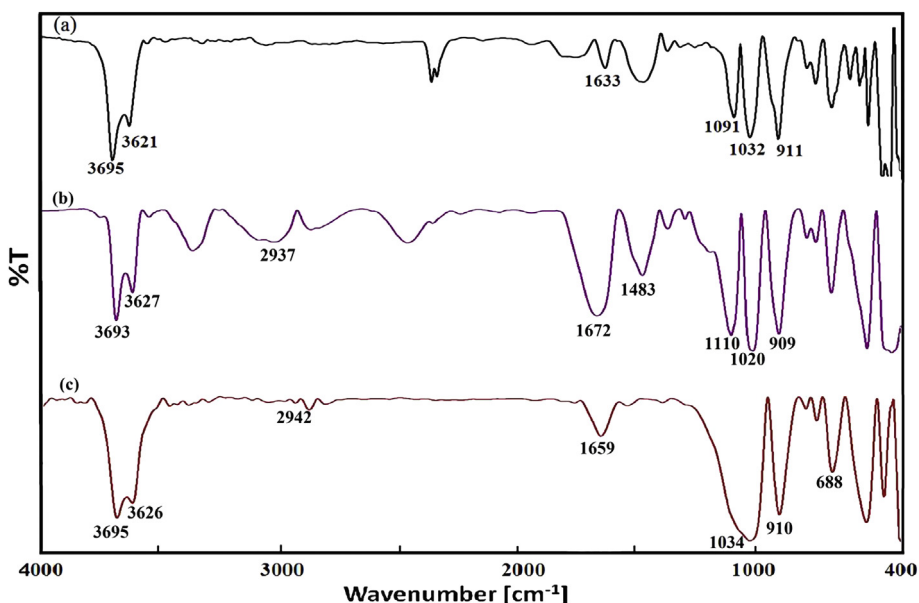


**Figure 5.** FTIR spectra (a) Halloysite Nanotubes (HNTs); (b) functionalized Halloysite Nanotubes (fHNT); (c) Silver immobilized HNT (HNT/Ag).

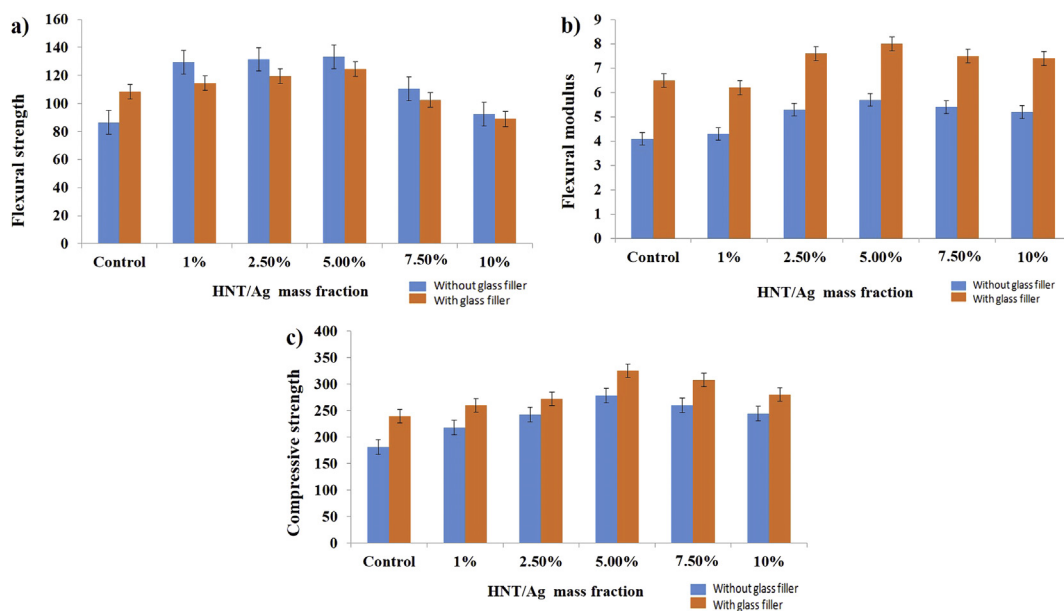


**Figure 6.** Mechanical properties of experimental resin composite with varied mass fraction of HNT/Ag (1%, 2.5%, 5%, 7.5% and 10%); (a) Flexural strength; (b) Flexural modulus; (c) Compressive strength; each bar represents the mean value of six samples, while the error bar represents one standard deviation ( $p < 0.05$ ).

properties. No major difference was found among the groups ( $p < 0.05$ ), thus, it can be inferred that the presence of different amounts of HNT/Ag did not affect the conversion of composites (Figure 7).

### 3.4.3. Curing depth

Curing depth depends on the duration of photo-polymerization and the intensity of a LED curing unit. To achieve enhanced mechanical properties of the dental resin composites, it is imperative that there is a higher conversion of the monomer to polymer. The results showed that curing depth decreases with increase in the amount of HNT/Ag filler, implying that a longer duration of curing is necessary to achieve a higher curing depth of the dental composite. The high refractive index (1.553–1.565) and opaque nature of HNT against the visible light results in lesser monomer conversion and low curing depth of dental resin composites [47]. However, these results still fulfil the requirements of clinical applications ( $>2.0$  mm) [48] (Figure 7).

### 3.4.4. Morphology of fractured dental composites

The fracture surfaces of the control group (H1), 2.5% HNT/Ag (H3), 5.0% HNT/Ag (H4) and 10% HNT/Ag (H6) were selected for SEM investigation. After the flexural tests, the fractured surfaces of composite were used in this study. The control group showed a smooth surface with oriented fracture lines originated due to the tensile stress. The fractured surface of the resin reinforced with 5% HNT/Ag (H4) displayed rough surface with no fracture lines. As the filler ratio increased in the composite, the surface roughness increased. The composite reinforced with 5% HNT/Ag (H4) showed very few agglomerations and exposed nanotubes. In contrast, the fractured surface of 10% HNT/Ag (H6) revealed more unevenness along with large agglomerates of the nanotubes. The agglomerates could act as a structural flaw that can weaken the resin composite. This reason can be attributed for the low mechanical strength of dental resin [49]. When compared with 5% HNT/Ag (H4); 10% HNT/Ag (H6) was less closely packed with non-uniform dispersion in

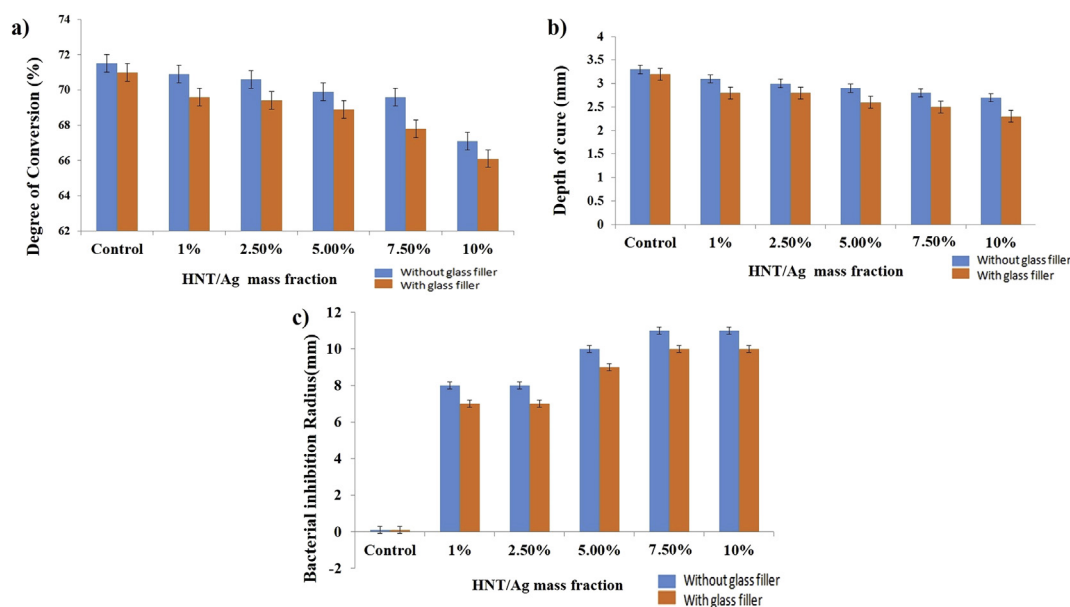


**Figure 7.** a) Degree of conversion (b) Depth of cure of resin composites with different amounts of HNT/Ag (1%, 2.5%, 5%, 7.5% and 10%) ( $p < 0.05$ ) (c) Bacterial inhibition radius ( $n = 3$ ,  $p < 0.05$ ).

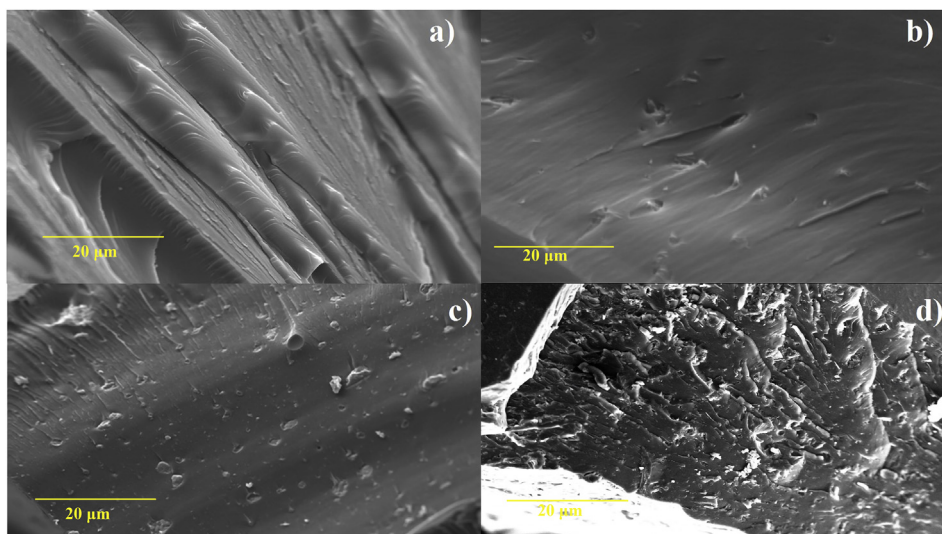


**Figure 8.** – Representative SEM images of fracture surfaces of the dental composites with different magnifications: (a) Control group (composite without fillers); (b) composite with 2.5% HNT/Ag; (c) composite with 5% HNT/Ag; and (d) composite with 10% HNT/Ag.

resin matrix. The presence of exposed nanotubes indicates poor interfacial adhesion and weak mechanical strength of the resin matrix studied (Figure 8).

### 3.4.5. Antimicrobial activity

In this study, antibacterial activity of HNT/Ag incorporated dental composites against *S. mutans* was evaluated. The antibacterial test showed that resin composites samples significantly inhibited bacterial growth, with higher concentration of HNT/Ag leading to a greater bacterial inhibition (Figure 7d). HNT did not show any bacterial activity as it inherently lacks any anti-bacterial properties. Also, significant difference was found in the inhibition efficiency between groups with different amounts of filler concentration, indicating that as the filler ratio in the composites increases, the zone of inhibition also increases [50] (Figure 7c).

These results showed that the inclusion of HNT/Ag (1–10 %) in the dental composite showed an effective antibacterial activity against *S. mutans*. The use of HNTs as a carrier may lead to sustained release of the agent, increasing antibacterial activity over time and with sufficient reduction in adverse effects against oral mucosal cells.

### 3.4.6. In-vitro cytotoxicity evaluation

The cytotoxicity of control (H1) and 5% HNT/Ag (H4) resin composite was evaluated through MTT assay. The extraction medium was cultured with NIH 3T3 fibroblast cells for 24, 48 and 72 h. As shown in Figure 9, the control group showed no significant cytotoxicity to the cells at 24, 48 and 72 h. It could be seen that the viability of cells treated with HNT/Ag resin composite was 76.5%, 83.7% and 96.5% at 24, 48 and 72 h, respectively. Subsequent increase in viability of cells with increase in time suggests biocompatibility of the composite. As reported earlier, average relative cell viability over 70%, is considered to be safe thereby attributing to the less toxic nature of the dental composite prepared. Also, addition of HNT/Ag did not cause any cytotoxicity indicating its future possible application for use in dentistry [19, 51] (Figure 9).

## 4. Discussion

Research on novel dental composites has been carried out continually to prolong the lifespan of composite restorations. The inclusion of antibacterial agents loaded nanofillers in dental resin may benefit restorative treatments by preventing bacterial colonization on tooth surface [6]. According to some earlier reports, the potential of HNT was explored to

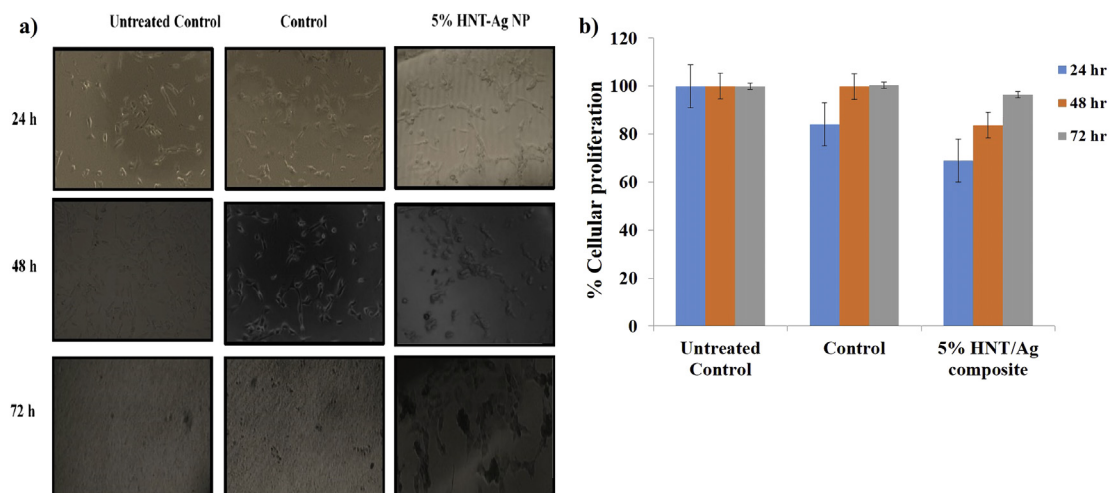


**Figure 9.** (a) Morphological changes; (b) Cellular proliferation in the composite treated on NIH-3T3 cell lines. X axis represents concentrations of compounds and Y-axis represents percent proliferation.



entrap a drug for a dental composite formation, however their mechanical properties were not in accordance with the commercial composites [8, 9, 10, 11, 17, 20, 29]. HNT was chosen due to its nanoscale size, nano tubular structure and due to the fact that it can be easily mixed with the dental resins for fabrication of composites [8]. In addition, immobilization of AgNPs on HNTs can be used to create a novel dental composite for different dental applications [21, 22, 23].

This study provides an in-depth analysis on new experimental dental composite comprising of HNT/Ag to provide antibacterial properties, without compromising mechanical strength. The morphological analysis using TEM displays the presence of AgNPs on outer surface of fHNT, confirming the successful immobilization of AgNPs.

In the current study, the incorporation of HNT/Ag (5%) in dental composite enhanced the mechanical properties and also exhibit significant antibacterial activity against *S. mutans*, the primary microorganism responsible for caries development. Also, the addition of higher amount of HNT/Ag (7.5 or 10%) increased the antimicrobial activity. However, these higher ratios of HNT/Ag in dental resin composite had weakening effect on the mechanical properties.

Considering HNT/Ag separately, this study presented that HNT/Ag at 10%, primarily affected the compressive strength of dental composite. However, a fall in the flexural as well as compression strength was noted when HNT/Ag and glass fillers were integrated together. Moreover, 10% HNT/Ag in resin matrix presented the best antimicrobial effects, however, they also presented the poorest performance in relation to mechanical strength.

The varied mass fraction of HNT/Ag in all the composites groups presented no major difference in DC values ( $p < 0.05$ ). These results display HNT/Ag in resin matrix did not affect their degree of conversion [45, 46]. Additionally, the silanol groups present on the outer surface of nanotubes may induce bioactivity for dental composites, and the tested groups presented values above 70% cell viability on NIH 3T3 cell lines confirming their promising biocompatibility [51, 52].

The addition of HNT/Ag into a dental resin composite resulted in long-term antibacterial properties compared to the commercially available dental composite. In addition, the immobilization of AgNPs on HNT did not interfere with its antimicrobial properties. In our study, disk diffusion method was used as it is relatively economical and can be executed quickly with many samples. The cytotoxicity of these new experimental dental resin composite was evaluated on NIH 3T3 cell lines showing its biocompatibility and non-toxic nature. It was observed that 5% HNT/Ag displayed the best results, probably due to uniform distribution of HNT/Ag fillers in resin composites. Incorporation of higher concentrations of HNT/Ag in resin matrix created clusters of HNTs that serves as the weakening point for the composite causing failure under stress and the mechanical tests results has confirmed it.

In this study, it was decided to incorporate HNT and Ag as an antibacterial agent simultaneously in the resin composite with the future goal of preventing bacterial colonization on tooth surface and increasing lifespan of the restoration. It was verified that the presence of HNTs did not interfere with the antimicrobial activity of Ag. Additionally, the inclusion of these agents in the resin matrix didn't have any negative impact on the mechanical strength of the dental composite. However, higher concentration of HNT/Ag (7.5 and 10%) had a pronounced negative influence on the mechanical strength, possibly due to the large cluster formation in the matrix of the composite [42, 43].

Additionally, cytotoxicity of the resultant experimental dental resin composite has shown a positive outcome on the cell viability with a significant increase over the time of study after an initial decrease at the end of 24 h time point [19, 32, 33]. The presence of HNT/Ag within the composition shows negligible cytotoxicity on NIH 3T3 cell lines without showing any negative effect on mechanical properties.

## 5. Conclusion

In conclusion, immobilization of Silver nanoparticle on outer surface of Halloysite Nanotubes (HNT/Ag) was successful. The results suggest that the mechanical strength was enhanced greatly after addition of HNT/Ag in dental resin matrix. Addition of HNT/Ag in the dental resins resulted in to superior antibacterial properties. Based on these results, the HNT/Ag filler based resin composites may be used as multipurpose restorative materials for potential dental applications. Among all composites, the composite with 5% HNT/Ag (H4) (without glass fillers) and 5% HNT/Ag (G4) (with glass fillers) offered the best and superior mechanical properties, excellent antimicrobial activity, and an acceptable curing depth and degree of conversion. Finally, the corresponding HNT/Ag based dental resin composites showed no significant cytotoxicity to NIH3T3 cell lines. The HNT/Ag filler in resin matrix certainly offers additional antimicrobial protection to dental composite. Therefore, HNT/Ag might be a hopeful as filler with antimicrobial properties for the development of robust dental composites for future applications in dentistry.

## Declarations

### Author contribution statement

Tejas Barot: Conceived and designed the experiments; Performed the experiments; Analyzed and interpreted the data; Wrote the paper.

Deepak Rawtani: Contributed reagents, materials, analysis tools or data; Wrote the paper.

Pratik Kulkarni: Performed the experiments; Analyzed and interpreted the data; Contributed reagents, materials, analysis tools or data; Wrote the paper.

### Funding statement

This research did not receive any specific grant from funding agencies in the public, commercial, or not-for-profit sectors.

### Competing interest statement

The authors declare no conflict of interest.

### Additional information

No additional information is available for this paper.

## References

- [1] J.L. Ferracane, Resin composite—state of the art, *Dent. Mater.* 27 (2011) 29–38.
- [2] F.F. Demarco, M.B. Corrêa, M.S. Cenci, R.R. Moraes, N.J. Opdam, Longevity of posterior composite restorations: not only a matter of materials, *Dent. Mater.* 28 (2012) 87–101.
- [3] L.A. Knobloch, R.E. Kerby, R. Seghi, J.S. Berlin, N. Clelland, Fracture toughness of packable and conventional composite materials, *J. Prosthet. Dent.* 88 (2002) 307–313.
- [4] K.D. Jandt, B.W. Sigusch, Future perspectives of resin-based dental materials, *Dent. Mater.* 25 (2009) 1001–1006.
- [5] P.C. Baehni, Y. Takeuchi, Anti-plaque agents in the prevention of biofilm-associated oral diseases, *Oral Dis.* (2003) 23–29.
- [6] Z. Khurshid, M. Zafar, S. Qasim, S. Shahab, M. Naseem, A. AbuReqaiba, *Advances in nanotechnology for restorative dentistry*, *Materials* 8 (2015) 717–731.
- [7] Y. Zheng, Y. Zheng, R. Ning, Effects of nanoparticles SiO<sub>2</sub> on the performance of nanocomposites, *Mater. Lett.* 57 (2003) 2940–2944.
- [8] D. Rawtani, Y.K. Agrawal, Multifarious applications of halloysite nanotubes: a review, *Rev. Adv. Mater. Sci.* 30 (2012) 282–295.
- [9] M. Du, B. Guo, D. Jia, Newly emerging applications of halloysite nanotubes: a review, *Polym. Int.* 59 (2010) 574–582.
- [10] H. Zhu, M. Du, M. Zou, C. Xu, Y. Fu, Green synthesis of Au nanoparticles immobilized on halloysite nanotubes for surface-enhanced Raman scattering substrates, *Dalton Trans.* 41 (2012) 10465–10471.
- [11] A. Saxena, R.M. Tripathi, R.P. Singh, Biological synthesis of silver nanoparticles by using onion (*Allium cepa*) extract and their antibacterial activity, *Dig. J. Nanomater. Bios.* 5 (2010) 427–432.

- [12] A. Panáček, L. Kvittek, R. Prucek, M. Kolář, R. Večeřová, N. Pizúrová, V.K. Sharma, T.J. Nevečná, R. Zbořil, Silver colloid nanoparticles: synthesis, characterization, and their antibacterial activity, *J. Mater. Chem. B* 110 (2006) 16248–16253.
- [13] K. Chaloupka, Y. Malam, A.M. Seifalian, Nanosilver as a new generation of nanoparticle in biomedical applications, *Trends Biotechnol.* 28 (2010) 580–588.
- [14] S. Silver, L.T. Phung, G. Silver, Silver as biocides in burn and wound dressings and bacterial resistance to silver compounds, *J. Ind. Microbiol. Biotechnol.* 33 (2006) 627–634.
- [15] S. Gurunathan, J.W. Han, D.N. Kwon, J.H. Kim, Enhanced antibacterial and anti-biofilm activities of silver nanoparticles against Gram-negative and Gram-positive bacteria, *Res. Lett.* 9 (2014) 373.
- [16] J.M. Corrêa, M. Mori, H.L. Sanches, A.D. Cruz, E. Poiate, I.A. Poiate, Silver nanoparticles in dental biomaterials, *Int. J. Biomater.* 2015 (2015).
- [17] M. Ai, Z. Du, S. Zhu, H. Geng, X. Zhang, Q. Cai, X. Yang, Composite resin reinforced with silver nanoparticles-laden hydroxyapatite nanowires for dental application, *Dent. Mater.* 33 (2017) 12–22.
- [18] Z. Shu, Y. Zhang, Q. Yang, H. Yang, Halloysite nanotubes supported Ag and ZnO nanoparticles with synergistically enhanced antibacterial activity, *Nanoscale Res. Lett.* 12 (2017) 1–7.
- [19] T. Barot, D. Rawtani, P. Kulkarni, C.M. Hussain, S. Akkireddy, Physicochemical and biological assessment of flowable resin composites incorporated with farnesol loaded halloysite nanotubes for dental applications, *J. Mech. Behav. Biomed. Mater.* 7 (2020) 103675.
- [20] G. Pandey, D.M. Mungambe, M. Tharmavaram, D. Rawtani, Y.K. Agrawal, Halloysite nanotubes-An efficient 'nano-support' for the immobilization of  $\alpha$ -amylase, *Appl. Clay Sci.* 136 (2017) 184–191.
- [21] S. Kumar-Krishnan, A. Hernandez-Rangel, U. Pal, O. Ceballos-Sanchez, F.J. Flores-Ruiz, E. Prokhorov, O.A. De Fuentes, R. Esparza, M. Meyyappan, Surface functionalized halloysite nanotubes decorated with silver nanoparticles for enzyme immobilization and biosensing, *J. Mater. Chem. B* 15 (2016) 2553–2560.
- [22] Y. Zhang, Y. Chen, H. Zhang, B. Zhang, J. Liu, Potent antibacterial activity of a novel silver nanoparticle-halloysite nanotube nanocomposite powder, *J. Inorg. Biochem.* 118 (2013) 59–64.
- [23] S. Jana, A.V. Kondakova, S.N. Shevchenko, E.V. Sheval, K.A. Gonchar, V.Y. Timoshenko, A.N. Vasiliev, Halloysite nanotubes with immobilized silver nanoparticles for anti-bacterial application, *Colloids Surf., B* 151 (2017) 249–254.
- [24] Z. Tarle, T. Attin, D. Marovic, L. Andermatt, M. Ristic, T.T. Tauböck, Influence of irradiation time on subsurface degree of conversion and microhardness of high-viscosity bulk-fill resin composites, *Clin. Oral Invest.* 19 (2015) 831–840.
- [25] H. Chadda, B.K. Satapathy, A. Patnaik, A.R. Ray, Mechanistic interpretations of fracture toughness and correlations to wear behaviour of hydroxyapatite and silica/hydroxyapatite filled bis-GMA/TEGDMA micro/hybrid dental restorative composites, *Compos. B Eng.* 130 (2017) 132–146.
- [26] F.J. Wegehaupt, N. Lunghi, G.N. Belibasakis, T. Attin, Influence of light-curing distance on degree of conversion and cytotoxicity of etch-and-rinse and self-etch adhesives, *BMC Oral Health* 17 (2017) 12.
- [27] D. Rawtani, G. Pandey, M. Tharmavaram, P. Pathak, S. Akkireddy, Y.K. Agrawal, Development of a novel 'nanocarrier' system based on Halloysite Nanotubes to overcome the complexation of ciprofloxacin with iron: an in vitro approach, *Appl. Clay Sci.* 150 (2017) 293–302.
- [28] D. Dai, M. Fan, Investigation of the dislocation of natural fibres by Fourier-transform infrared spectroscopy, *Vib. Spectrosc.* 55 (2011) 300–306.
- [29] S.A. Feitosa, J. Palasuk, K. Kamocki, S. Geraldini, R.L. Gregory, J.A. Platt, L.J. Windsor, M.C. Bottino, Doxycycline-encapsulated nanotube-modified dentin adhesives, *J. Dent. Res.* 93 (2014) 1270–1276.
- [30] A. Tsujimoto, W.W. Barkmeier, T. Takamizawa, M.A. Latta, M. Miyazaki, Mechanical properties, volumetric shrinkage and depth of cure of short fiber-reinforced resin composite, *Dent. Mater. J.* 35 (2016) 418–424.
- [31] L.S. Türkün, M. Türkün, F.A. Ertuğrul, M. Ates, S. Brugger, Long-term antibacterial effects and physical properties of a chlorhexidine-containing glass ionomer cement, *J. Esthetic Restor. Dent.* 20 (2008) 29–44.
- [32] S. Imazato, T. Imai, R.R. Russell, M. Torii, S. Ebisu, Antibacterial activity of cured dental resin incorporating the antibacterial monomer MDPB and an adhesion-promoting monomer, *J. Biomed. Mater. Res.: Off. J. Soc. Biomater., J. Biomed. Mater. Res. A* 39 (1998) 511–515.
- [33] K. Hotwani, N. Thosar, S. Baliga, S. Bundale, K. Sharma, Antibacterial effects of hybrid tooth colored restorative materials against *Streptococcus mutans*: an in vitro analysis, *J. Conserv. Dent.* 16 (2013) 319.
- [34] P. Kulkarni, D. Rawtani, T. Barot, Formulation and optimization of long acting dual niosomes using Box-Behnken experimental design method for combinative delivery of Ethionamide and D-cycloserine in Tuberculosis treatment, *Colloids Surf., A* 565 (2019) 131–142.
- [35] H. Li, X. Zhu, H. Zhou, S. Zhong, Functionalization of halloysite nanotubes by enlargement and hydrophobicity for sustained release of analgesic, *Colloids Surf., A* 487 (2015) 154–161.
- [36] D. Rawtani, Y.K. Agrawal, A study of the behavior of HNT with DNA IntercalatorAcridine orange, *BioNanoSci* 3 (2013) 52–57.
- [37] M. Tharmavaram, G. Pandey, D. Rawtani, Surface modified halloysite nanotubes: a flexible interface for biological, environmental and catalytic applications, *Adv. Colloid Interface Sci.* 261 (2018) 82–101.
- [38] D. Rawtani, Y.K. Agrawal, Study of nanocomposites with emphasis to halloysite nanotubes, *Rev. Adv. Mater. Sci.* 32 (2012) 149–157.
- [39] K. Shamel, M.B. Ahmad, A. Zamanian, P. Sangpour, P. Shabanzadeh, Y. Abdollahi, M. Zargar, Green biosynthesis of silver nanoparticles using *Curcuma longa* tuber powder, *Int. J. Nanomed.* 7 (2012) 5603.
- [40] P. Yuan, P.D. Southon, Z. Liu, M.E. Green, J.M. Hook, S.J. Antill, C.J. Kepert, Functionalization of halloysite clay nanotubes by grafting with  $\gamma$ -aminopropyltriethoxysilane, *J. Phys. Chem. C* 112 (2008) 15742–15751.
- [41] J. Saadat S, M. Tharmavaram, G. Pandey, V. Braganza, D. Rawtani, Nano-interfacial decoration of Halloysite Nanotubes for the development of antimicrobial nanocomposites, *Adv. Colloid Interface Sci.* 275 (2020) 102063.
- [42] K. Prashantha, M.F. Lacrampe, P. Krawczak, Processing and characterization of halloysite nanotubes filled polypropylene nanocomposites based on a masterbatch route: effect of halloysites treatment on structural and mechanical properties, *Express Polym. Lett.* 5 (2011).
- [43] M. Liu, Y. Zhang, C. Wu, S. Xiong, C. Zhou, Chitosan/halloysite nanotubes bionanocomposites: structure, mechanical properties and biocompatibility, *Int. J. Biol. Macromol.* 51 (2012) 566–575.
- [44] A. Alhuthali, I.M. Low, Water absorption, mechanical, and thermal properties of halloysite nanotube reinforced vinyl-ester nanocomposites, *J. Mater. Sci.* 48 (2013) 4260–4273.
- [45] K.H. Chung, E.H. Greener, Correlation between degree of conversion, filler concentration and mechanical properties of posterior composite resins, *J. Oral Rehabil.* 17 (1990) 487–494.
- [46] M. Eldiwany, J.M. Powers, L.A. George, Mechanical properties of direct and post-cured composites, *Am. J. Dent.* 6 (1993) 222–224.
- [47] N. Ilie, Comparative Effect of self-or dual-curing on polymerization kinetics and mechanical properties in a novel, dental-resin-based composite with alkaline filler, *Materials* 11 (2018) 108.
- [48] S. Rooj, A. Das, V. Thakur, R.N. Mahaling, A.K. Bhowmick, G. Heinrich, Preparation and properties of natural nanocomposites based on natural rubber and naturally occurring halloysite nanotubes, *Mater. Des.* 31 (2010) 2151–2156.
- [49] M.C. Bottino, G. Batarseh, J. Palasuk, M.S. Alkathiri, L.J. Windsor, J.A. Platt, Nanotube-modified dentin adhesive—physicochemical and dentin bonding characterizations, *Dent. Mater.* 29 (2013) 1158–1165.
- [50] S. Satish, M. Tharmavaram, D. Rawtani, Halloysite nanotubes as a nature's boon for biomedical applications, *Nanomedicine* 6 (2019).
- [51] W. Kangwansupamonkon, V. Laurungtana, S. Surassmo, U. Ruktanonchai, Antibacterial effect of apatite-coated titanium dioxide for textiles applications, *Nanomedicine* 5 (2009) 240–249.
- [52] X. Miao, Y. Li, Q. Zhang, M. Zhu, H. Wang, Low shrinkage light curable dental nanocomposites using SiO<sub>2</sub> microspheres as fillers, *Mater. Sci. Eng. C* 32 (2012) 2115–2121.